

Electron tunneling and noise studies in ferromagnetic junctions

E.R. Nowak^{a,*}, P. Spradling^b, M.B. Weissman^b, S.S.P. Parkin^c

^a*Department of Physics & Astronomy, University of Delaware, Newark, DE 19716, USA*

^b*Department of Physics, University of Illinois, Urbana, IL 61801, USA*

^c*IBM Research Division, Almaden Research Center, San Jose, CA 95120, USA*

Abstract

Transport properties of exchange-biased magnetic tunnel junction structures are reported as a function of tunnel barrier thickness. The temperature dependence of the tunneling conductance and magnetoresistance (MR) is consistent with recent theories relating it to the magnon excitations at the electrode–barrier interface or the temperature-dependent surface magnetization. We have also measured the bias voltage dependence of the MR. For CoFe magnetic electrodes, the reduction in MR is approximately 50% at biases of ~ 250 mV. At low temperatures, we observe a cusp-like dip in the tunneling conductance at zero-bias. The conductance increases as the square-root of the bias voltage, indicating that electron–electron interactions as in disordered media may be important. Coating a magnetic electrode or the oxide barrier with an alternate, thin magnetic layer of higher spin polarization is shown to generally increase the MR by several percent but at the expense of higher $1/f$ noise. © 2000 Elsevier Science B.V. All rights reserved.

Keywords: Tunnelling; Magnetic structures; Magnetoresistance; Electrical properties and measurements

1. Introduction

Tunneling magnetoresistance in magnetic tunnel junctions (MTJs) is of fundamental interest [1] and potentially applicable to magnetic sensors and memory devices [2]. In 1970, spin polarized tunneling experiments by Meservey and Tedrow [3,4], showed that the conduction electrons in ferromagnetic (FM) materials are spin polarized and the spin is conserved in the tunneling process. The spin polarization, P , of a ferromagnet is associated with its unequal spin distribution at the Fermi level. Julliere's model [5] for FM-insulator-FM tunneling, predicts that the tunnel junction magnetoresistance (MR) is

$$\text{MR} \equiv \frac{R_{AP} - R_P}{R_P} = \frac{2P_1P_2}{1 - P_1P_2},$$

where P_1 and P_2 are the spin polarization of the two FM electrodes. R_{AP} and R_P are the tunneling resistances when the top and bottom FM electrodes are magnetized parallel and antiparallel relative to one another. The tunneling resistance depends on the relative orientation because of the asymmetry in the density of states of the majority and minority energy bands in a ferromagnet. For example, in the parallel orientation the number of occupied states in one electrode and available states in the other electrode are well matched. Hence, the tunneling current is at a maximum and the tunneling resistance is a minimum. On the other hand, the mismatch in the number of majority states in one electrode and minority states in the other electrode results in a minimum of current and a maximum of resistance. Half-metallic compounds, such

* Corresponding author. Tel.: +1-302-831-2676; fax: +1-302-831-1637.

E-mail address: nowak@udel.edu (E.R. Nowak).

NiMnSb, Fe_3O_4 , CrO_2 and the perovskite manganites, would in principle show an infinite MR due to their 100% spin-polarized Fermi surfaces.

The Julliere model works rather well at predicting the magnitude of the MR seen in high quality junctions. However, it disregards important points such as impurity scattering, magnon excitations, and defect assisted tunneling processes. Experimental studies show that the MR exhibits both a temperature and a d.c. bias dependence [1]; features that are not accounted for by Julliere model. These effects are significant and depend on the quality of the junction. In this work, we address a number of issues like these, including the electrical noise properties of MTJs and the origin of the peak in the tunneling resistance at zero bias.

2. Magnetic tunnel junction materials

Ferromagnetic tunnel junctions are made in the form of a multilayered film deposited on a Si wafer in a d.c. magnetron sputtering vacuum system; details have been published elsewhere [2,6]. Individual layers are deposited through a series of metal shadow masks. The masks allow 10 tunnel junctions to be grown simultaneously across each 1.0 inch diameter Si wafer; each junction has a cross-geometry pattern with area $A \approx 55 \times 55 \mu\text{m}^2$. The deposition takes place in the presence of a 100 Oe magnetic field directed in the plane of the film to induce uniaxial magnetic anisotropy. The final heterostructure is made in situ without breaking vacuum and is given by $\text{Si}/\text{SiO}_2/5\text{Ti}/15\text{Pd}/10\text{Mn}_{46}\text{Fe}_{54}/3\text{Co}_{84}\text{Fe}_{16}/\text{Al}_2\text{O}_3/8\text{Co}_{84}\text{Fe}_{16}/20\text{Pd}/5\text{Ti}$ where the numbers represent the nominal layer thickness in nanometers. The insulating Al_2O_3 barrier is formed by plasma oxidizing a layer of Al metal prior to depositing the remaining layers. Hence, tunneling occurs between the two CoFe layers. Junctions were grown with Al metal thickness, d , ranging from 1.2 to 3.0 nm. The oxidation conditions were held constant at 100 mTorr and a 4-min duration for all the junctions. Although the fraction of oxidized Al metal was not determined, we expect complete oxidation of the Al and some oxidation of the bottom FM layer for small d , whereas for large d some Al metal may remain unoxidized. For a set of junctions having $d = 2.0$ nm, an additional thin layer of Fe was deposited either on top of the Al_2O_3 layer or underneath the Al metal prior to oxidation.

For non-volatile memory applications it is favorable to have two stable magnetic states in zero applied magnetic field. This property is achieved by utilizing FM layers with different magnetic coercivities so that the relative orientations of the magnetic moments can be changed. In our MTJs the antiferromagnetic MnFe layer magnetically 'pins' the lower FM layer by ex-

change bias. The top CoFe layer has a low coercive field and forms the 'free' FM layer.

Measurements of the magnetoresistance, differential tunneling resistance ($R_d = dV/dI$), and voltage noise were performed using a conventional four-probe technique. The magnetic field, H , was applied in the plane of the junction and collinear with the easy axis.

3. Results and discussion

Fig. 1 (inset) shows a typical resistance vs. field curve for an MTJ with $d = 1.8$ nm. This MTJ has an MR $\sim 38\%$ at room temperature and a resistance $R_P \sim 3.8$ k Ω , corresponding to a specific resistance $R_s = R_P \times A = 11.5$ M Ω (μm^2). The low resistance state reflects the parallel (P) alignment of the magnetization vectors in the two FM layers, whereas antiparallel (AP) alignment results in a higher tunneling resistance. Only the magnetization of the top FM layer is free to switch orientations at low fields; switching fields can range from a few to tens of Oersteds. The magnetic switching of the free layer is single-domain-like; the typical width of the transition is less than 1 Oe for $d > 2$ nm for which the effects of dipolar coupling and incomplete oxide coverage are reduced [7]. The pinning of the exchange biased FM layer is overcome at high fields which restores parallel alignment. The corresponding drop in MR occurs at $H = 600$ Oe for the MTJ in Fig. 1. The pinned layer's broad transition is presumably due to the flipping of many domains.

The effects of Al metal overlayers on the room-temperature magnetoresistance [7,8] and $1/f$ noise [8] have been discussed previously. In an effort to increase the

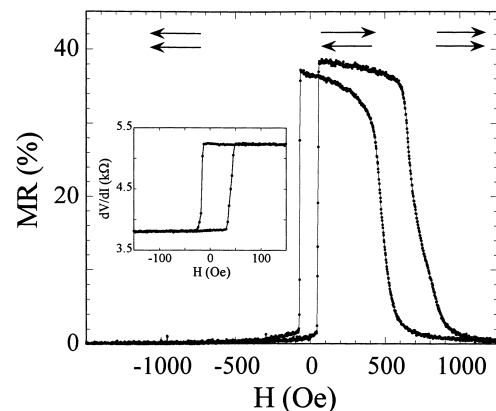


Fig. 1. Room temperature magnetoresistance vs. field curve for a MTJ with a 1.8 nm Al metal layer forming the oxide tunneling barrier. The main panel shows the variation in the MR ratio caused by the switching of the free FM layer near zero field as well as the switching of the exchange biased FM layer at ~ 600 Oe. The arrows represent the corresponding relative orientations of the magnetic moments in the two FM layers. The inset shows the low-field magnetoresistance curve in greater detail.

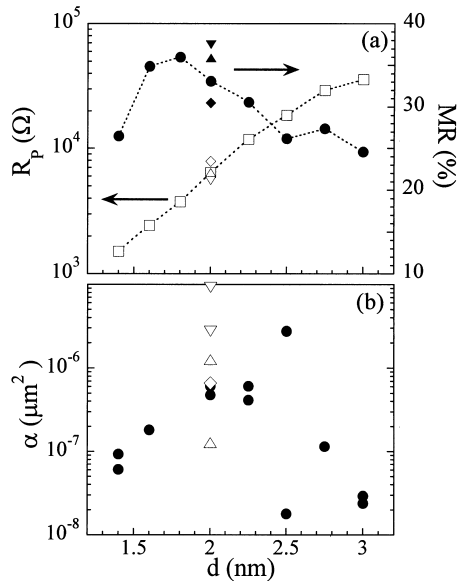


Fig. 2. Panel (a) shows the average resistance (open symbols) and average MR (solid symbols) measured at zero-bias as a function of Al metal thickness. The dependence of the normalized $1/f$ noise on Al metal thickness is shown in (b). The effect of depositing a 0.25 nm (\blacktriangle , \triangle) and 0.5 nm (\blacktriangledown , \triangledown) thick Fe layer below an Al metal layer and a 2-nm (\blacklozenge , \lozenge) thick Fe layer on top of an oxidized Al metal layer is shown for $d = 2.0$ nm. All data is for $T = 295$ K.

MR we investigated the effects of depositing a thin layer of magnetic material (iron) with a higher spin polarization at the FM-barrier interfaces. The results with and without a Fe layer at $d = 2$ nm are shown in Fig. 2. Without the Fe layer, the MR (averaged over several nominally identical junctions) exhibits a broad peak at $d = 1.8$ nm. A lower spin polarization and, hence, a lower MR is expected if unoxidized Al remains on the surface of the bottom FM at higher d , or if the underlying FM surface becomes oxidized for thinner Al overlayers [7].

Compared to the variation with Al thickness, an Fe layer has little effect on the junction resistance. However, a 2.0-nm thick layer of Fe deposited on top of the Al_2O_3 lowered the MR by 7%. If the Fe layer is placed below the Al metal then the MR actually increases, by as much as 13% for a 0.5-nm thick Fe underlayer. For another set of junctions with a 0.25-nm Fe underlayer we found a 6% enhancement in the MR. We are uncertain as to why the MR increases if the Fe layer is positioned below the Al metal, since this potentially exposes it to oxidation. The reason may involve a combination of effects including stoichiometry, morphology, and interface properties.

Tunnel junctions under constant current bias exhibit voltage fluctuations. The power spectrum of these fluctuations is comprised of a frequency independent component (current shot noise and Johnson noise) and a $1/f$ part, where f is the frequency [8,9]. The $1/f$ power spectrum scales as the mean current squared. Its origin

has been attributed to resistance fluctuations arising from charge trapping processes [8,10]. The degree to which the $1/f$ noise arises from charge trapping inside the tunnel barrier or at the FM-insulator boundary is revealed by examining the dependence of noise magnitude on the Al layer thickness. Fig. 2b shows that the normalized noise, given by $\alpha = fS_R A / R_d^2$ where S_R is the power spectral density of the resistance fluctuations, exhibits a broad peak near $d = 2$ nm. The coincidence at $d \geq 2.5$ nm of the onset of sub-exponential dependence of R_d on d in Fig. 2a with the dramatic drop in α , shown in Fig. 2b, indicates that an oxidized Al-FM interface is a major source of noise [8].

Generally, a Fe underlayer increases the MR but at the expense of higher noise. Fig. 2b shows that junctions with a 0.5 nm Fe underlayer have noise magnitudes that are a factor of 5–20 times larger than those without a Fe layer (solid symbols). The junction with the Fe layer deposited on top of the Al_2O_3 had nominally the same α as junctions without the Fe layer, whereas for one junction having a 0.25-nm Fe underlayer, α was found to be smaller. Among nominally identical junctions having the same Fe layer (open symbols in Fig. 2b) there was considerably more variation in α than was observed for nominally identical junctions without a Fe layer (solid symbols in Fig. 2b). One exception is for the two nominally identical junctions having $d = 2.5$ nm for which α differs by a factor of 100. These two junctions and all those with Fe layers were studied one year after the others. It may be possible that over this period of time the barrier and interface properties were altered due to oxygen migration or diffusion of chemical species — a type of aging effect. Additional studies to attain better statistics are desirable.

A distinctive feature of MTJs is the decrease in magnetoresistance with increasing temperature [1]. Fig. 3d shows that the reduction in the zero-bias MR in our MTJs can be as large as 25% between 2 and 300 K. This decrease in MR could come from thermally activated conduction that is spin-independent or from the smearing of the Fermi surface. Our findings are consistent with recent theoretical [11,12] and experimental studies [13] that relate the reduction of the MR to the reduced spin polarization that is proportional to the T -dependent saturation moment, $m_s(T) \sim -T^{3/2}$. The dashed line in Fig. 3d is a fit to the predicted temperature dependence [12]: $\text{MR}(T) = \text{MR}(T=0)(1-AT^{3/2})$. The fitting parameter, A , was of order $\sim 10^{-5} \text{ K}^{-3/2}$ for several samples. Satisfactory fits (dashed lines in Fig. 3c) can also be obtained to the predictions of a model [11] that relates $\text{MR}(T)$ to electron-magnon scattering. In this case, the zero-bias tunneling conductance, $G(V=0) = dI/dV$, is predicted to increase as $T \log T$ for both P and AP orientations. On the basis of these fits, and others on more detailed data (not shown),

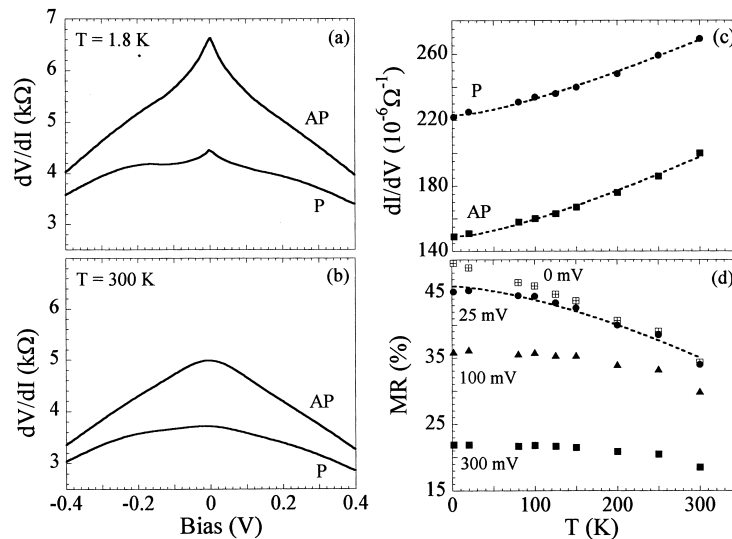


Fig. 3. In (a) and (b), the differential resistance of a junction having $d = 1.8$ nm is plotted as a function of d.c. bias at two temperatures for the parallel (P) and antiparallel (AP) orientation of the magnetizations. For the same junction, the temperature dependence of the zero-bias differential conductance is shown in (c) and the MR ratio in (d). The dashed lines are fits to theories discussed in the text.

it is not possible to distinguish between these two models.

MTJs exhibit a substantial decrease in MR with the application of bias, see Fig. 3d. The large reduction in MR, nearly 50% at biases ~ 250 mV, can be accounted for by the stronger bias dependence of the tunneling resistance in the AP state. The differential resistance of one of our junctions is plotted in Fig. 3a,b at two temperatures. Although $R_d(V)$ has the general feature of a metal–insulator–metal tunnel junction [14], the detailed shape of the curve shows deviations from simple calculations such as Simmons’s formula at all temperatures. For example, at room temperature $R_d(V)$ has somewhat of a linear trend at biases greater than a few $k_B T$, particularly in the AP state. For identical tunneling electrodes, $R_d(V)$ is expected to be symmetric about zero-bias. The asymmetry we observe is most pronounced at small d , and may reflect differences in the electrode–barrier interfaces due to partial oxidation of the bottom CoFe electrode. Particularly when the bottom electrode is negatively biased there is a slight increase in resistance observed at ~ -200 mV. This feature is most prominent for the P orientation in Fig. 3a,b. For $T < 100$ K a resistance peak develops in the $R_d(V)$ spectrum at $V = 0$, as shown in Fig. 3a. This zero-bias anomaly is surprisingly robust; it is evident for all the junctions studied and typically dominates $R_d(V)$ up to 100 mV.

The bias dependence of the MR is not well understood [1]. A decrease of MR is obtained in a simple Slonczewski-type parabolic band model [15–17] in which the bias shifts the electrode band towards higher density of states. The initial reduction at low biases, however, is much slower than observed [13]. Other factors,

such as excitation of magnons and an energy dependence of spin polarization due to the band structure, have been proposed. Recent calculations [11,12] show that a significant part of the reduction in MR can be attributed to magnon excitations, as also seen from inelastic tunneling spectra [13]. Moreover, Zhang et al. [11] have attributed the zero bias anomaly to magnon excitations at the electrode–barrier interface. In general, the dip in conductance at $V = 0$ can be expected to be due to some combination of effects that include: the presence of magnons, magnetic impurities, interface states, and multi-step tunneling through states in the barrier (including ones from metal particles). Next, we examine an alternate possibility for the origin of the zero-bias anomaly.

It has been shown that in disordered systems, when the electronic mean free path is comparable to the wavelength, the electron–electron interaction leads to a repulsion in the density of states symmetric about the Fermi energy [18]. In the limit of strong scattering the predicted density of states variation is given by [18,19] $N(E) = N(0)(1 + \sqrt{E/\Delta})$, where Δ is a pseudo-correlation gap, an energy corresponding to the screening length. With increasing disorder, the screening length diverges and Δ collapses to zero. Since the tunneling conductance is proportional to $N(E)$, this singularity in turn leads to a $V^{1/2}$ dependence of the tunneling conductance.

In Fig. 4 we plot the tunneling conductance, $(dI/dV)/\sigma_0$, (normalized by the zero-bias conductance) as a function of the square root of the bias voltage of the tunnel junction ($V^{1/2}$). The temperature dependence of $G(V)$ for a selected junction is shown in Fig. 4a. In Fig. 4b we plot the low temperature ($T < 10$

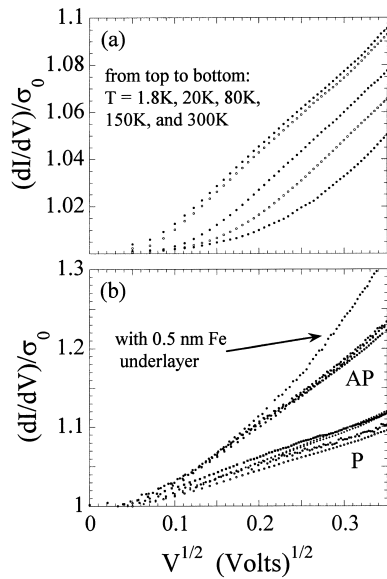


Fig. 4. The normalized differential conductance $(dI/dV)/\sigma_0$ is plotted as a function of \sqrt{V} . In (a), data is shown at various temperatures for the same junction as in Fig. 3 in the parallel orientation. In (b), the low-temperature ($T < 10$ K) conductance curves are shown for junctions having $d = 1.8, 2.0, 2.25, 2.75, 3.0$ nm in both magnetic orientations. Also, the effect of Fe-doping on the conductance is shown for a junction having a 2-nm thick Al layer in the antiparallel orientation.

K) $G(V)$ curves for junctions having various Al metal thicknesses. Insofar as these are straight lines at the higher biases, it supports the presence of a pseudogap. We think that the rounding of the $G(V)$ curves at small biases in Fig. 4 is due to thermal smearing (a few $k_B T$) of the pseudogap at $T \neq 0$. Deviations from the \sqrt{V} dependence occur at biases higher than those shown in Fig. 4, and for a junction having a thin Fe underlayer, see Fig. 4b. The slopes of the linear portions of these curves are a measure of $1/\Delta$. Δ depends weakly on temperature (Fig. 4a) and Al metal thickness (Fig. 4b). The relative magnetic state of the electrodes, however, has a significant effect; $\Delta \approx 1.2$ eV in the AP orientation which is roughly a factor of 2 smaller than in the P orientation.

Tunneling measurements have shown a \sqrt{V} dependence of the density of states near the metal–insulator transition in granular aluminum [20] and amorphous $\text{Ge}_{1-x}\text{Au}_x$ films [21]. However, the CoFe magnetic electrodes in our MTJs are good metals with low resistivity. Since tunneling electrons come from the top few monolayers of the FM film, a plausible explanation for the zero-bias anomaly in $G(V)$ in our junctions may be that it is due to a disorder-induced renormalization of the surface density of states due to electron–electron interactions. If so, the weak dependence of Δ on d is somewhat surprising. Apparently the oxidation condition of the bottom Al–FM interface does not change

the character of the disorder. It is interesting to note corroborating evidence from experimental studies of colossal magnetoresistance magnetic tunnel junctions grown by molecular beam epitaxy. In that work, a zero bias anomaly is observed in $G(V)$ at low temperatures, the strength of which is correlated with the quality of the growth as judged by reflective high energy electron diffraction (RHEED) [22].

What does this mean for the large difference in Δ observed in the AP and P configurations? It is difficult to understand how a disorder-induced singularity in the density of states can be so strongly affected by changing the magnetic state. If Δ is taken as a measure of disorder than the smaller value of Δ in the AP state implies that it is *more* disordered. We are uncertain as to the origin of this effect. One possibility is that minority carriers in the AP orientation have a smaller correlation gap due to their lower concentration. A smaller carrier density implies a lower conductance channel. The smaller value of Δ in the AP state would then be consistent with the corresponding larger screening length due to the lower conductance. The extent to which the zero-bias anomaly is due to Coulomb effects in the dirty limit or other factors, such as multi-step tunneling, remains elusive.

4. Conclusion

Detailed tunneling and noise studies as a function of temperature and dc bias in high MR junctions reveal some of the fundamental phenomena in FM–I–FM tunnel junctions. The temperature dependence of the MR and tunneling conductance are consistent magnon excitations near the surface of the FM electrodes, although based on these data it is not possible to distinguish between competing models for the reduction of the MR with increasing temperature. From the point of view of applications, the reduction in MR with increasing bias and the avoidance of oxidation of the FM–Al interfaces in minimizing the $1/f$ noise are of great importance. It is not clear to what extent magnon scattering is a complete explanation of the bias dependence of the MR or the zero-bias anomaly observed in the tunneling conductance. In the latter case, we observe a \sqrt{V} dependence of the density of states. This behavior may indicate that disorder and electron correlation effects play a significant role in shaping the conductance spectrum at low biases, perhaps even up to room temperature.

Acknowledgements

It is a pleasure to thank J. Ecstein and J. O'Donnell for many valuable discussions. Experimental work was

done at the University of Illinois and was supported in part by DARPA under Contract No. MDA972-96-C-0030 and by the NSF through Grant No. DMR 96-23478.

References

- [1] J.S. Moodera, G. Mathon, *J. Magn. Magnetic Mater.* 200 (1999) 248.
- [2] S.S.P. Parkin, K.P. Roche, M.G. Samant et al., *J. Appl. Phys.* 85 (1999) 5828.
- [3] R. Meservey, P.M. Tedrow, P. Fulde, *Phys. Rev. Lett.* 18 (1970) 1270.
- [4] R. Meservey, P.M. Tedrow, *Phys. Rep.* 238 (1994) 173.
- [5] M. Julliere, *Phys. Lett.* 54 (1975) 225.
- [6] W.J. Gallagher, S.S.P. Parkin, X.P. Bian et al., *J. Appl. Phys.* 81 (1997) 3741.
- [7] J.S. Moodera, E.F. Gallagher, K. Robinson et al., *Appl. Phys. Lett.* 70 (1997) 3050.
- [8] E.R. Nowak, M.B. Weissman, S.S.P. Parkin, *Appl. Phys. Lett.* 74 (1999) 600.
- [9] G. Lecoy, L. Gousskov, *Phys. Status Solidi* 30 (1968) 9.
- [10] E.R. Nowak, R.D. Merithew, M.B. Weissman et al., *J. Appl. Phys.* 84 (1998) 6195.
- [11] S. Zhang, P.M. Levy, A.C. Marley et al., *Phys. Rev. Lett.* 79 (1997) 3744.
- [12] A.H. MacDonald, T. Jungwirth, M. Kasner, *Phys. Rev. Lett.* 81 (1998) 705.
- [13] J.S. Moodera, J. Nowak, R.J.M. van de Veerdonk, *Phys. Rev. Lett.* 80 (1998) 2941.
- [14] E.L. Wolf, *Principles of Electron Tunneling Spectroscopy*, Oxford University Press, New York, 1985.
- [15] J.C. Slonczewski, *Phys. Rev. B* 39 (1989) 6995.
- [16] A.M. Bratkovsky, *Phys. Rev. B* 56 (1997) 2344.
- [17] X. Zhang, B.-Z. Li, G. Sun et al., *Phys. Rev. B* 56 (1997) 5484.
- [18] B.L. Altshuler, A.G. Aronov, *Solid State Commun.* 30 (1979) 115.
- [19] W.L. McMillan, *Phys. Rev. B* 24 (1981) 2739.
- [20] R.C. Dynes, J.P. Garno, *Phys. Rev. Lett.* 46 (1981) 137.
- [21] W.L. McMillan, J. Mochel, *Phys. Rev. Lett.* 46 (1981) 556.
- [22] J. O'Donnell, A.E. Andrus, S. Oh et al., *Appl. Phys. Lett.* 76 (2000) 1914.